

An Overview of Research at HKU on HSRC Columns and Beam-Column Joints for Low-Medium Seismic-Risked Regions

H.J. Pam¹, J.C.M. Ho¹ J. Li²

The University of Hong Kong, HKSAR, PRC¹, Email: pamhoatjoen@hku.hk

South China University of Technology, Guangzhou, PRC²

ABSTRACT: Up to now building structures in Hong Kong (HK) are not required to resist earthquake effects. The design is based primarily on strength without taking into account any ductility consideration. Therefore, the resulting structures would have unpredictable inelastic performance when subject to overloading, a sudden impact or an earthquake attack. The situation is even worse if the structural members are of high-strength reinforced concrete (HSRC), which is becoming more popular in HK. To improve the post-elastic design of reinforced concrete (RC) members, a continued research study consisting of experimental tests has been conducted at The University of Hong Kong (HKU) since 2000, which covered among others tests on HSRC columns and internal RC beam-column joints. This paper reviews these research studies that focused on the strength, ductility and reinforcement detailing of columns and internal beam-columns joints. The test results showed that HSRC columns and beam-column joints designed according to the authors' proposals behaved in a limited ductile manner, which is suitable for low-medium seismic-risked regions where HK is located.

KEYWORDS: beam-column joint, ductility, high-strength reinforced concrete, low-medium seismic risk

1 INTRODUCTION

In spite of her location within a low-medium seismic zone [GB50011-2001], Hong Kong (HK) has no requirements for seismic design for building structures. Current design of RC structures in HK that covers high-strength concrete relies mostly on flexural strength provisions to resist gravity and wind loads at the ultimate limit state and on stiffness provisions to limit the maximum deflection at the serviceability limit state [BD 2004]. Although inherent minimum ductility exists due to some deem-to-satisfy rules, it has been shown by previous research that the above provisions could not ensure adequate members' flexural ductility [Ho & Pam 2002 & 2003; Ho 2003]. The members so designed behaved from very brittle to slightly ductile depending on the axial load level. Furthermore, no guidelines were given for the reinforcement design and detailing of beam-column joints in the design code adopted prior to 2008 in HK [BS8110-1985, Huang 2003, Li 2003; Au *et al* 2005]. Therefore, a review on the flexural ductility design of RC members was considered necessary in HK. The focus of this study is on HSRC columns and beam-column joints.

The design philosophy adopted in seismic countries relies on the energy dissipation in RC members through extensive inelastic deformation occurred within their critical regions. To allow energy dissipation to happen under large deformation while maintaining a reasonable flexural capacity, adequate confinement steel should be provided within the critical region to avert brittle failure. As for beam-column joints, additional steel should be installed to resist shear force due to lateral loads. Nevertheless in regions of low-medium seismic risk like HK, design provision for full ductility would create unnecessary steel congestion within joints as well as critical regions in beams and columns. It is believed that the transverse steel content in these regions could be reduced while maintaining a moderate level of flexural ductility. The design of limited ductile columns and joints was the focus of research in The University of Hong Kong (HKU).

Since the last decade, as part of HKU commitment to promote awareness of earthquake resistant design and detailing in HK, several series of experimental research have been conducted, among others were on HSRC columns [Ho 2003] and interior

beam-column joints [Huang 2003, Li 2003] to investigate the performance of these structural members under earthquakes. A total number of 20 HSRC columns and 27 interior beam-column joints were subjected to low frequency cyclic displacement simulating earthquake induced inertia. Due to page limitation, this paper only focuses on the tests of 15 HSRC columns and 10 beam-column joints.

For HSRC columns, the flexural ductility performance of column specimens designed complying with BS8110 [1985] was investigated. A parametric study based on nonlinear moment-curvature analyses was carried out. From the parametric study, an equation was proposed for the design of confinement steel content within the critical region. Subsequently, column specimens designed according to the proposed equation were fabricated and tested. The test results showed that the group of columns designed according to the proposed equation behaved in a limited ductile manner.

For HSRC interior beam-column joints, two joint reinforcing details were proposed: (1) additional diagonal steel; and (2) continuous diagonal steel. Interior beam-column joint specimens installed with the above details were fabricated and tested. The test results were compared with those obtained from the counterpart specimens without joint reinforcement (i.e. "empty joint") and with stirrups. It was apparent that beam-column joints containing the proposed joint details behaved in a limited ductile manner, i.e. more ductile than the "empty joint" and slightly less ductile than the specimen containing stirrups. Under compressive axial loading, the specimens containing additional as well as continuous diagonal steel had flexural ductility performance comparable to that of joint specimens containing stirrups.

A summary of proposed design guidelines for HSRC columns and interior beam-column joints is presented.

2 EXPERIMENTAL PROGRAMME

2.1 Test set-up

All the column and beam-column joint specimens were tested in a 660-tonne self-reaction steel loading frame under various compressive axial load levels and reversed cyclic inelastic displacement. Figures 1(a) and 1(b) show the respective typical set-up.

Each column in Figure 1(a) represents the column length in a multi-storey building between the mid-height and beam-column interface. The area of interest is the column region in the proximity of the interface. Cyclic bending moment was applied by two

hydraulic actuators to the column through the rigid beam and the axial load was applied by another hydraulic actuator underneath the bottom hinge.

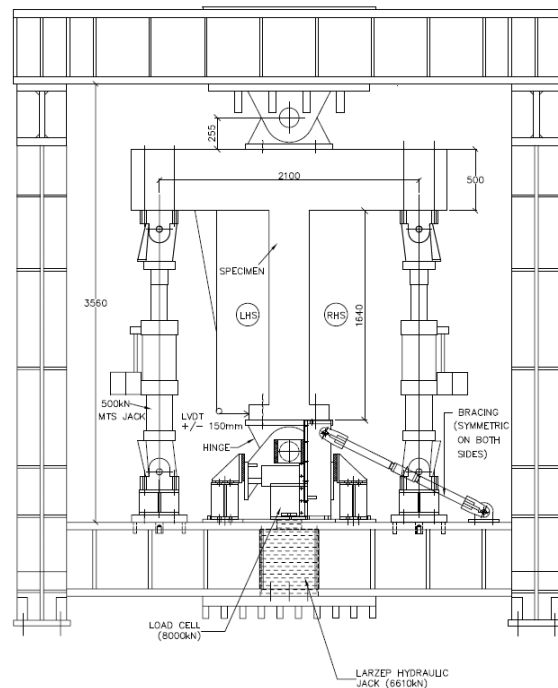


Figure 1(a). Typical setup for column specimens

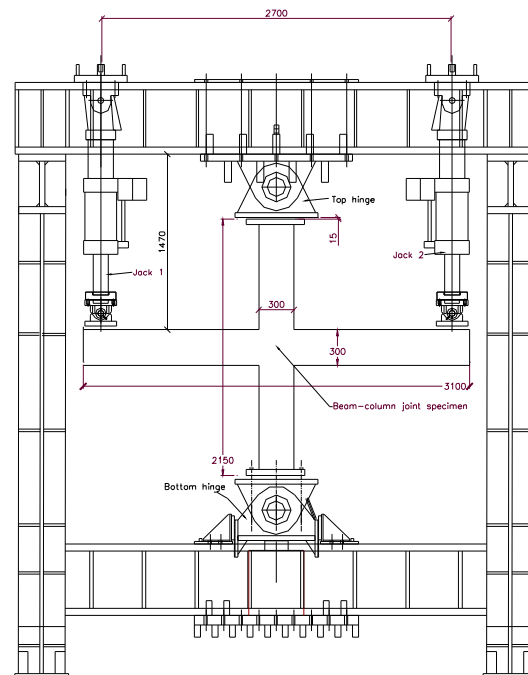


Figure 1(b). Typical setup for beam-column joint specimens

Figure 2 shows the isometric view of the column specimens and the typical details of stirrups in BS specimens.

The beam-column joint assemblage represents a typical interior beam-column joint of a multi-storey framed building bounded by contra-flexure points in

the adjacent members. Cyclic bending moment and compression axial load were applied in the similar manner explained for the column specimens.

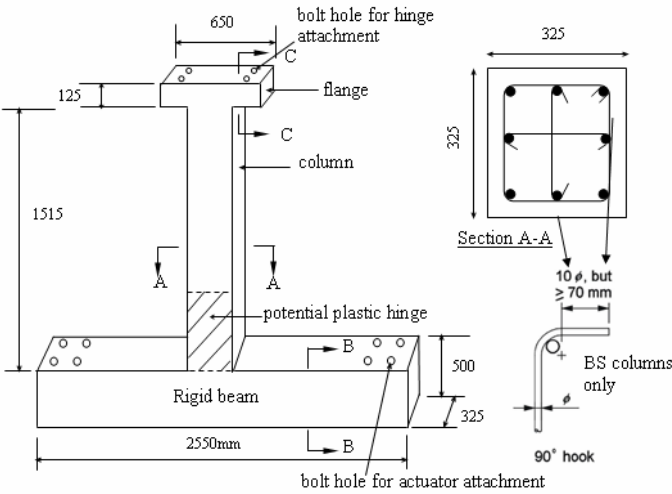
was increased to $\pm\Delta_y$, reaching $\mu = \pm 1$ respectively, where μ is nominal displacement ductility factor written as:

$$\mu = \frac{\Delta}{\Delta_y} \quad (2)$$

The process was repeated until the measured moment capacity is less than 80% of the measured peak moment M_p .

2.3 Instrumentation

The instrumentation installed in all the specimens was: (1) strain gauges, i.e. to measure bending strains in the longitudinal steel and, shear as well as confining strains in the transverse steel; and (2) linear variable displacement transducers (LVDT), i.e. to measure column and beam curvature profiles, column rotations and column tip deflections. Figures 3a and 3b show the instrumentation arrangement for respectively column and beam-column joint specimens.



Note: all dimensions in mm

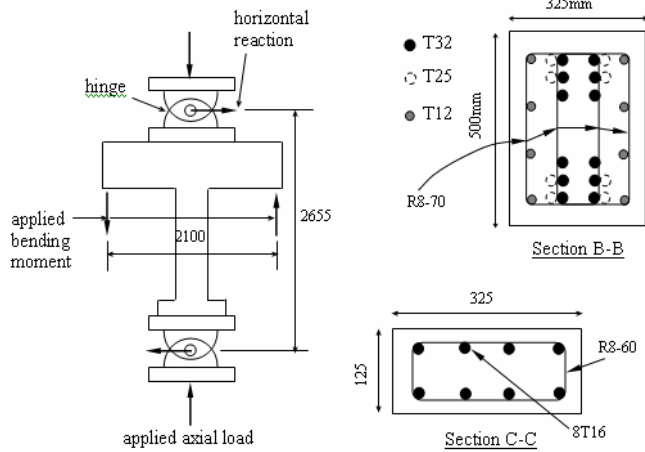


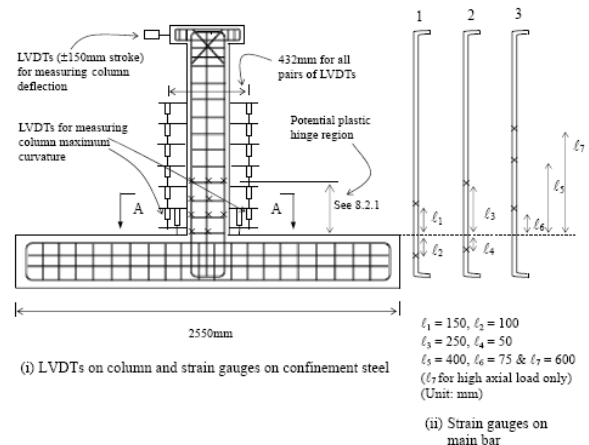
Figure 2. Perspective view of column specimens

2.2 Test procedure

The test was divided into load- and displacement-controlled cycles. In the first and only load-controlled cycle, the actuator loads were applied to produce $\pm 0.75M_u$ at the beam-column interface, where M_u is the column or beam (for beam-column joint specimens) flexural strength calculated by BS8110 [1985]. The respective displacements at the column tip or beam ends were recorded as Δ_1 and Δ_2 , from which the nominal yield displacement Δ_y could be determined by:

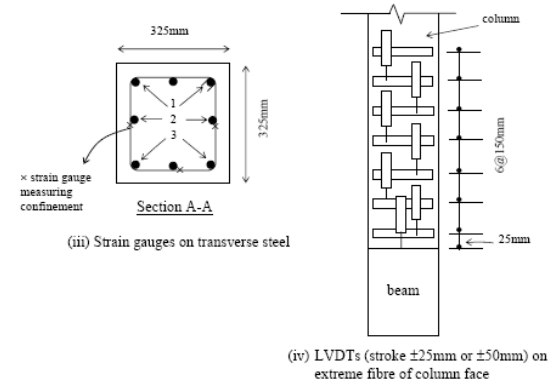
$$\Delta_y = \frac{4}{3} \left(\frac{\Delta_1 + |\Delta_2|}{2} \right) \quad (1)$$

The subsequent cycles were displacement-controlled. In the second cycle, the column lateral displacement or beam end vertical displacement (Δ)



(i) LVDTs on column and strain gauges on confinement steel

(ii) Strain gauges on main bar



(iv) LVDTs (stroke ±25mm or ±50mm) on extreme fibre of column face

Figure 3(a). Strain gauge and LVDT arrangement of column specimens (continued)

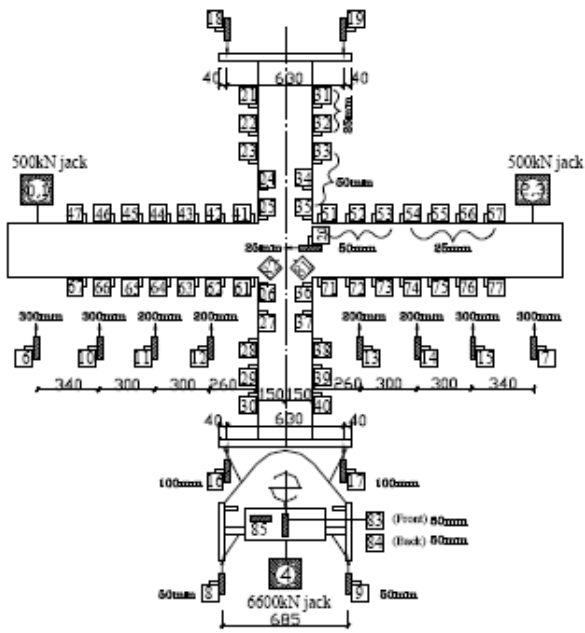


Figure 3(b). LVDT arrangement of beam-column specimens

3 TEST RESULTS OF HSRC COLUMNS

3.1 Details of column specimens

Tables 1a and 1b summarize the section properties and axial load levels of the column specimens. The transverse steel provided in the critical region of the “NEW” column was designed according to the proposed Equation (3) and provided with 45° or also known as 135 end hooks.

$$\rho_s = \left(\frac{A_g}{A_c} \right) \left(0.2 - 0.2 \frac{\rho f_y}{f_{cu}} \right) \left(\frac{P}{A_g f_{cu}} \right)^{0.9} \left(\frac{f_{cu}}{f_{ys}} \right) + 0.008 \quad (3)$$

where ρ_s is volumetric ratio of transverse steel, A_g and A_c are gross and core concrete areas respectively, ρ is the longitudinal steel ratio, f_{cu} is concrete cube strength, f_y and f_{ys} are yield strengths of respectively longitudinal and transverse steels and P is axial load.

Table 1a. Section properties of NEW column specimens

Unit	Actual f_{cu} (MPa)	Average $P/A_g f_{cu}$	Longitudinal steel		Transverse steel within potential plastic hinge region				
			Content ρ (%)	d (mm)	s (mm)	ρ_s (%)	ρ_s' (%)	ρ_s'' (%)	
NEW-60-06-61-S	57.1 (50.0)	0.53	ST32	6.1	T12 (R6)	70 (100)	2.10 (0.38)	1.95	1.64
NEW-60-06-61-C	62.4 (56.1)	0.53	ST32	6.1	T12 (R8)	110 (210)	2.00 (0.47)	1.95	1.64
NEW-100-03-24-S	96.5 (83.3)	0.28	ST20	2.4	T12 (R8)	70 (100)	2.10 (0.66)	2.38	2.30
NEW-100-03-24-C	108.4 (96.4)	0.34	ST20	2.4	T12 (R8)	90 (150)	2.45 (0.66)	2.38	2.30
NEW-80-01-09-S	85.9 (77.8)	0.11	ST12	0.9	R12 (R6)	85 (100)	1.73 (0.38)	1.71	1.40
NEW-80-03-24-C	90.4 (80.6)	0.28	ST20	2.4	T12 (R8)	105 (150)	2.10 (0.66)	2.03	1.92
NEW-100-03-61-C	108.8 (94.7)	0.30	ST32	6.1	T12 (R8)	100 (100)	2.20 (1.00)	2.10	1.85
NEW-100-06-61-C	100.0 (85.0)	0.55	ST32	6.1	T16 (R8)	120 (100)	3.20 (1.00)	3.20	2.60

The yield strength of high yielded deform bar (T) and mild steel round bar (R) are respectively 530 and 350MPa.

Table 1b. Section properties of BS column specimens

Unit	Actual f_{cu}/f'_c (MPa)	Average $P/A_g f_{cu}$	Longitudinal steel		Transverse steel within potential plastic hinge region		
			Content ρ (%)	d (mm)	s (mm)	ρ_s (%)	
BS-60-06-61-S	56.5/51.1	0.54	ST32	6.1	R6	100	0.38
BS-60-06-61-C	60.4/53.2	0.53	ST32	6.1	R8	210	0.47
BS-100-03-24-S	95.1/82.8	0.28	ST20	2.4	R8	100	0.66
BS-100-03-24-C	109.5/87.5	0.31	ST20	2.4	R8	150	0.66
BS-80-01-09-S(1)	89.6/75.0	0.11	ST12	0.9	R6	100	0.38
BS-80-01-09-S(2)	85.4/74.6	0.11	ST12	0.9	R8	175	0.38
BS-80-01-09-S(3)	83.2/72.4	0.11	ST12	0.9	R10	220	0.47

The yield strength of high yielded deform bar (T) and mild steel round bar (R) are respectively 530 and 350MPa.

Outside the critical region, the transverse steel was designed according to the shear requirement and the end hooks were 90°.

3.2 Flexural ductility performance of NEW columns

Figure 4 shows the moment - lateral displacement and moment-curvature hysteresis curves of a pair of NEW and BS columns. The theoretical moment is marked by a horizontal line, whereas the dotted inclined line marks the loss due to $P-\Delta$ effect. Failure of column is defined at $0.8M_p$ post-peak. It is also shown the scales of actual displacement ductility factor μ' obtained by substituting the respective parameters in Equations (1) and (2) by those at $0.75M_p$. The ultimate displacement ductility factors (μ_d) and ultimate curvature ductility factor (μ_c) are defined as:

$$\mu_d = \Delta_u / \Delta_y' \quad (4a)$$

$$\mu_c = \phi_u / \phi_y \quad (4b)$$

$$\phi_y = \phi_y' / 0.75 \quad (4c)$$

where Δ_u and ϕ_u are respectively the measured column displacement and curvature at failure. ϕ_y' is the measured column curvature at $0.75M_p$ pre-peak.

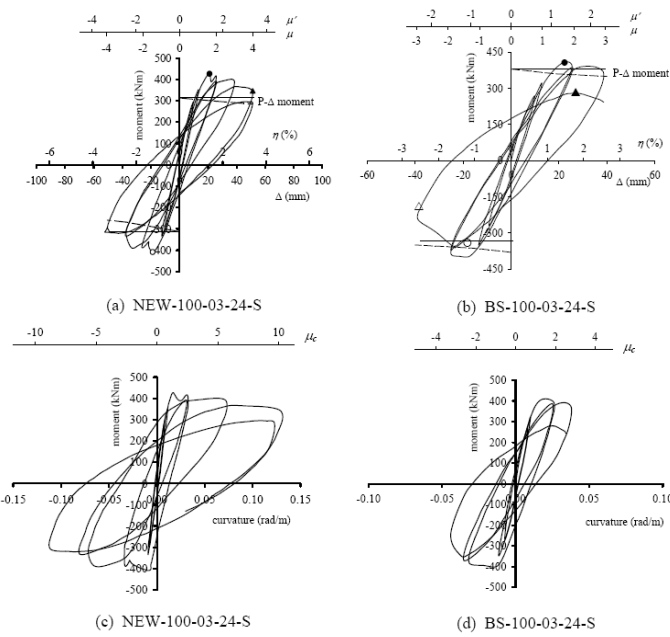


Figure 4. Moment – lateral displacement and -curvature hysteresis curves of NEW-100-03-24-S and BS-100-03-24-S

Table 2. Results of NEW and BS column specimens

Unit	Δ_y (mm)	Δ_y' (mm)*	Δ_u (mm)	μ_d	ϕ_y (rad/m)*	ϕ_u (rad/m)	μ_c
NEW-60-06-61-S	14.0	20.4	68.6	3.4	0.0149	0.1230	8.3
NEW-60-06-61-C	15.7	20.0	79.9	4.0	0.0171	0.1742	10.2
NEW-100-03-24-S	12.5	15.3	51.7	3.4	0.0127	0.1205	9.5
NEW-100-03-24-C	15.2	18.9	73.7	3.9	0.0125	0.1121	9.0
NEW-80-01-09-S	10.7	18.4	67.1	3.7	0.0175	0.2233	12.8
NEW-80-03-24-C	14.7	18.4	77.5	4.2	0.0151	0.1481	9.8
NEW-100-03-61-C	20.0	24.4	108.2	4.4	0.0153	0.1726	11.3
NEW-100-06-61-C	12.3	19.9	89.7	4.5	0.0188	0.1944	10.4
BS-60-06-61-S	14.4	16.8	30.5	1.8	0.0228	0.0529	2.3
BS-60-06-61-C	16.8	19.1	38.9	2.0	0.0220	0.0522	2.4
BS-100-03-24-S	12.7	16.7	34.4	2.1	0.0135	0.0387	2.9
BS-100-03-24-C	17.1	16.9	27.5	1.6	0.0127	0.0210	1.7
BS-80-01-09-S(1)	11.1	16.8	54.2	3.2	0.0244	0.1769	7.3
BS-80-01-09-S(2)	13.1	20.1	53.8	2.7	0.0195	0.1400	7.2
BS-80-01-09-S(3)	11.8	20.0	53.5	2.7	0.0222	0.1700	7.7

From Figure 4, it is concluded that NEW columns (1) have a higher flexural strength; (2) can undergo many more inelastic cycles; and (3) behave in a limited ductile manner by reaching $\mu_c \approx 10$. Table 2 summarizes the results.

A common phenomenon observed in all the BS columns was the opening of 90° end hooks of stirrups within the critical region. This was however not observed in the NEW columns having 135° end hooks. Furthermore, it was found that the longitudinal steel buckled in a double-curvature manner, which proved that the 135° end hooks effectively restrained the longitudinal bars from buckling. It therefore increased the buckling load of the longitudinal steel and delayed the inelastic buckling. Figure 5 shows this phenomenon.

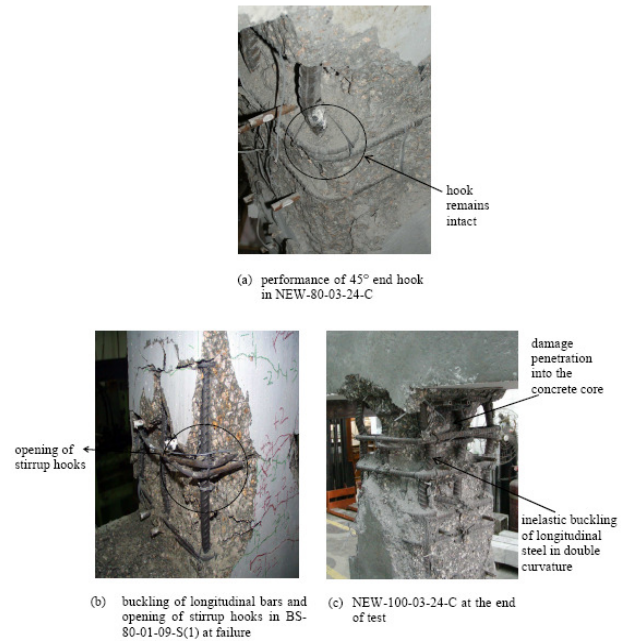


Figure 5. Some observed behaviour in column specimens

3.3 Effect of transverse steel configuration

The $M-\Delta$ and $M-\phi$ hysteresis curves of a similar pair of BS and NEW columns containing internal cross ties are shown in Figure 6. It is seen that the addition of cross ties increases the ultimate deformability of the limited ductile column specimen substantially, i.e. NEW-100-03-24-S could only achieve $\eta = \pm 3.7\%$ (where $\eta = \text{drift}$) while NEW-100-03-24-C could achieve $\eta \geq \pm 6.0\%$. Nevertheless, it reduces the ductility in non-ductile columns, i.e., BS-100-03-24-S reached $\mu = 3$ with $\eta = 2.7\%$, whereas BS-100-03-24-C could only reach $\mu = 2$ with $\eta = 2.0\%$. It is also observed that cross ties with 135° end hooks were effective in restraining the longitudinal steel since it buckled in a double curvature manner, while those with 90° end hooks were pushed open by the buckled longitudinal steel. Table 2 summarizes the values of μ_d and μ_c for these columns.

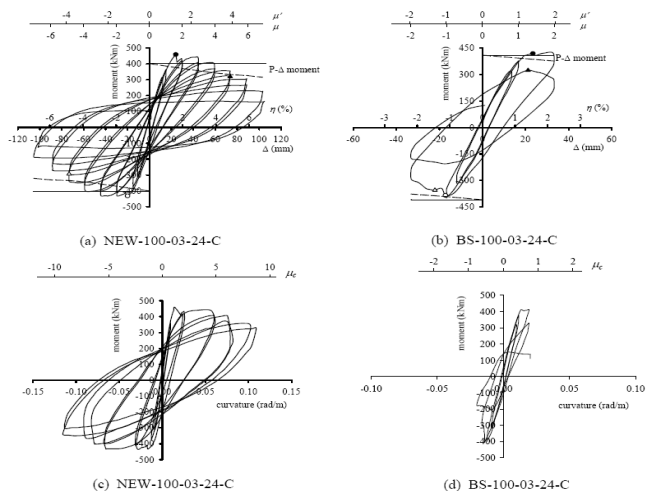


Figure 6. Moment – lateral displacement and moment-curvature hysteresis curves of NEW-100-03-24-C and BS-100-03-24-C

3.4 Critical region length

The critical region length refers to the extent of region from the maximum bending moment point that suffers extensive inelastic damage [Park & Paulay 1975; Watson & Park 1994; Mendis 2001] and therefore needs to be confined. In this paper, the critical region length in each HSRC column was evaluated based on physical observation and measured curvature profile. In the former, the critical region length is defined by the region suffering buckling of longitudinal steel and damage penetration into concrete core. Some of them are shown in Figure 7 and all are listed in Table 3. In the latter method, the critical region length is defined as the length of column having curvature at the ultimate state larger than the yield value. The results are also listed in Table 3.

Table 3. Critical region lengths for column specimens

Unit	ϕ_y (rad/m)	ℓ_p based on physical observation (mm)		ℓ_p based on curvature profile (mm)	
		LHS/RHS	Average	+ve/-ve	Average
NEW-60-06-61-S	0.0149	400/400	400	480/480	480
NEW-60-06-61-C	0.0171	300/300	300	340/440	390
NEW-100-03-24-S	0.0127	450/450	450	480/440	460
NEW-100-03-24-C	0.0125	400/350	375	455/500	478
NEW-80-01-09-S	0.0175	250/250	250	300/300	300
NEW-80-03-24-C	0.0151	320/320	320	460/500	480
NEW-100-03-61-C	0.0153	450/450	450	600/500	550
NEW-100-06-61-C	0.0188	620/620	620	680/650	665
BS-60-06-61-S	0.0228	550/550	550	520/520	520
BS-60-06-61-C	0.0218	600/600	600	500/500	500
BS-100-03-24-S	0.0135	650/650	650	540/440	490
BS-100-03-24-C	0.0127	630/630	630	500/420	460
BS-80-01-09-S(1)	0.0244	270/250	260	280/280	280
BS-80-01-09-S(2)	0.0195	220/260	240	290/290	290
BS-80-01-09-S(3)	0.0222	260/260	260	260/260	260

Note: LHS = left hand side ; RHS = right hand side

4 TEST RESULTS OF HSRC BEAM-COLUMN

Figure 8 and Table 4 summarise the sectional properties of all the beam-column joint specimens.

4.1 Existing design of beam column joint – “empty joint” and “with stirrups”

The first type of beam-column joint specimen is the “empty joint” (denoted as “E specimen”), which contained nothing in the joint apart from the longitudinal steel from the beams and columns. This is the common design practice in countries having low-medium seismic risk like HK. However, research [Huang 2003, Li 2003, Au *et al* 2005] has shown that empty joints were insufficient to resist lateral shear forces induced by moderate earthquakes. The specimens of this series serve as the reference

specimens having flexural ductility performance at the lower bound.

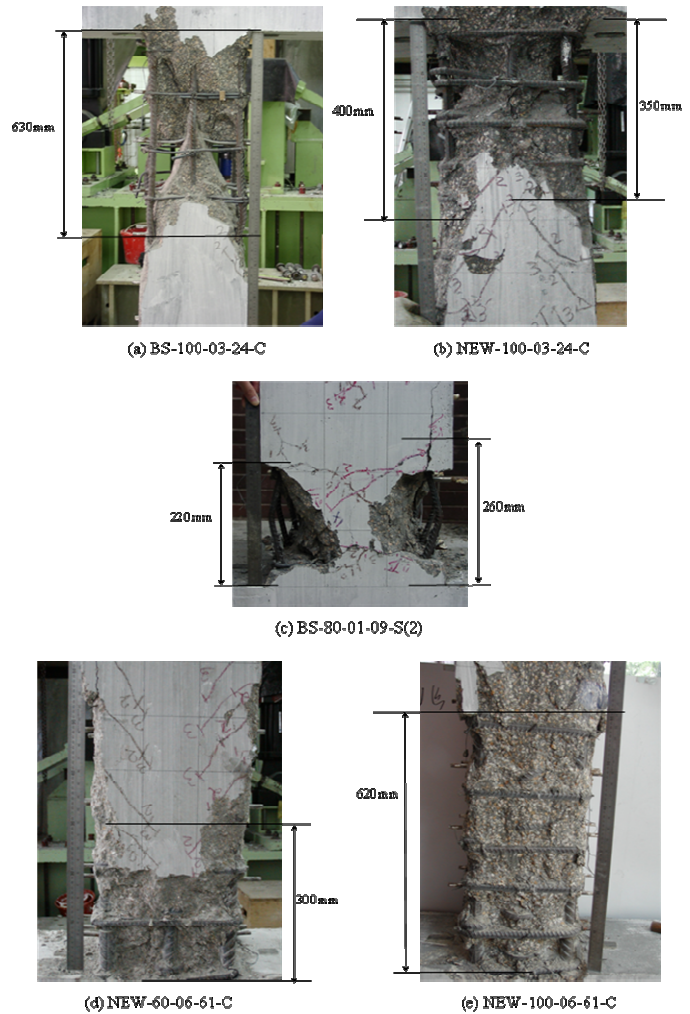


Figure 7. Some observed critical regions

Table 4. Section properties of beam-column joint specimens

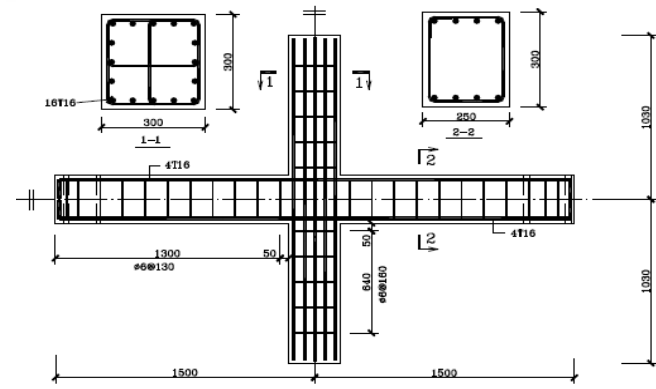
Unit	Joint detail	f_{cu} / f'_c (MPa)		Stirrups	
		Beam	Column	Beam	Column
E-C80-B80-0	Empty	88.2/79.7	88.2/79.7	nominal	nominal
E-C80-B40-0.2	Empty	50.6/45.2	87.2/76.9	nominal	nominal
H-C80-B80-0	3-3T12	82.7/75.7	82.7/75.7	nominal	nominal
H-C80I-B80I-0.6	3-3T12	90.8/80.1	90.8/80.1	improved	improved
AD-C80-B80-0	2T16	86.7/78.5	86.7/78.5	nominal	nominal
AD-C80-B80I-0	2T16	79.7/68.5	79.7/68.5	improved	nominal
AD-C80I-B80I-0.6	2T16	84.2/77.0	84.2/77.0	improved	improved
AD-C80I-B80M-0.6	2T16	79.8/68.0	79.8/68.0	modified	improved
CD-C80-B80-0	2T16	82.5/79.0	82.5/79.0	nominal	nominal
CD-C80-B40-0.3	2T16	48.2/40.5	86.1/79.5	nominal	nominal

Notes: - Yield strengths of high yielded deform bar (T) and mild steel round bar (R) are respectively 550 and 370MPa.

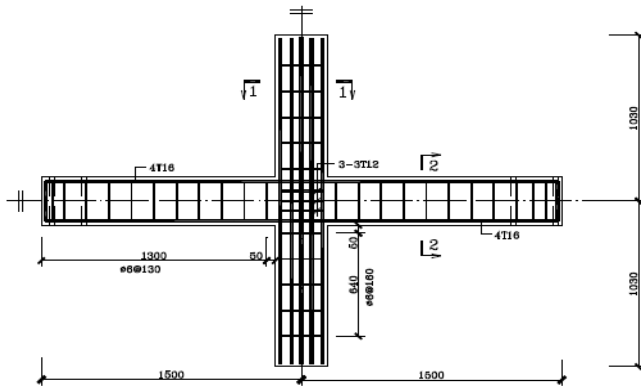
- Nominal stirrups are calculated according to shear resistance requirement.

- Improved stirrups contained more stirrups and installed in critical regions only.

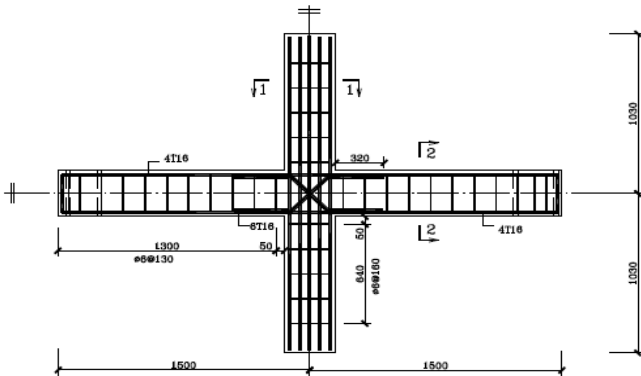
- Modified stirrups contained more stirrups and installed in whole length of beams.



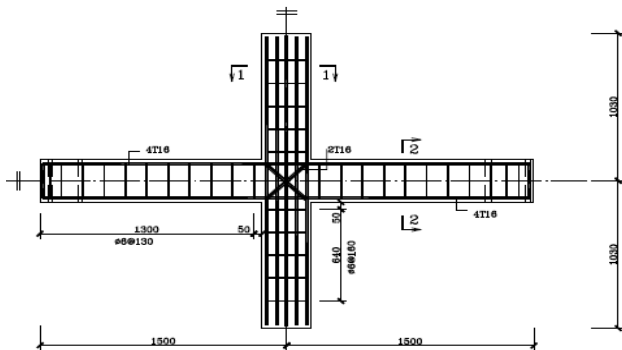
(a) E specimen ("empty joint")



(b) H specimen ("stirrups")



(c) AD specimen ("additional diagonal bars")



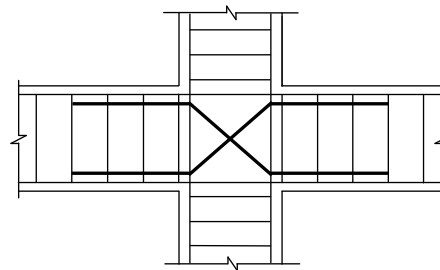
(d) CD specimen ("continuous diagonal bars")

The second type of specimen contained stirrups within the joint (denoted as "H specimen"). This detail is commonly adopted in countries subjected to high seismic risk and the structural members are expected to behave fully ductile. Nonetheless, this joint detail often creates steel congestion problem in the joint and fabrication difficulties in reinforcement caging. The specimens in this series serve as another reference having flexural ductility performance at the upper bound.

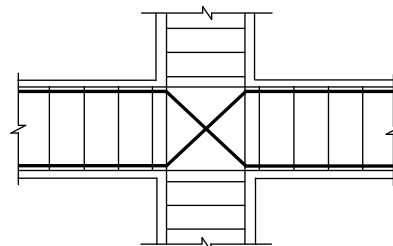
4.2 Proposed joint details

The purpose of this research study is to propose alternative joint details suitable for RC frames located in low-medium seismic-risked regions and at the same time reduce the joint steel congestion. Beam-column joints containing the proposed details (Figure 9) are expected to behave in a limited ductile manner, i.e. their flexural ductility falls within the lower and upper bounds.

The first proposed joint detail is additional diagonal steel in the form of "obtuse Z" in two opposite directions (denoted as "AD specimen"). The length of the horizontal tail projecting out from each side of the column face was set at about one-half of its full development length calculated from BS8110 [1985], and the inclined component aligns with the joint diagonally. Figure 9a shows the elevation detail of AD specimen. The amount of diagonal steel was designed based on the joint shear force as required by NZS 3101 [1995].



(a) Additional diagonal steel



(b) Continuous diagonal steel

Figure 9. Proposed joint details

The second proposed joint detail is in the form of continuous diagonal steel. The detail is similar to the

Figure 8. Reinforcement details in beam-column specimens

additional diagonal steel, except the diagonal bars were bent from the inner beam longitudinal bars (denoted as “CD specimen”). Figure 9b shows the elevation detail of CD specimen. The remaining unbent longitudinal bars in the beam will run through the joint.

4.3 Behaviour of joints without axial load

Figure 10 shows the response of column shear force (V_c) versus column displacement (Δ) as well as column drift (η) for Units E-C80-B80-0, H-C80-B80-0, AD-C80-B80-0, AD-C80-B80I-0 and CD-C80-B80-0. The theoretical shear strength of the column is V_n and marked as dotted line in the figure. Each joint specimen contained similar material strengths and section properties for easy comparison, except more stirrups were added within the beam critical region of Unit AD-C80-B80I-0. From the figure, it is observed that the E and CD specimens only managed to reach the respective theoretical strength, while the others (H and AD specimens) achieved higher strength than their respective theoretical strength. The largest strength enhancement ratio was obtained in Unit AD-C80-B80I-0 (~26%) due to a better confinement in its beams. The strength enhancement ratios for other specimens are summarised in Table 5.

Table 5. Test results of beam-column joints without axial load

Specimen	M_n (kNm)	Failure mode	Actual/nominal strength ratio	At failure	
				μ	drift (%)
E-C80-B80-0	114.6	Joint brittle failure	0.97	3.0	5.1
H-C80-B80-0	114.2	Beam flexural shear failure	1.06	3.6	6.3
AD-C80-B80-0	114.5	Beam shear failure	1.15	3.5	4.9
AD-C80-B80I-0	117.9	Joint ductile failure	1.26	4.0	6.4
CD-C80-B80-0	114.2	Joint ductile failure	0.98	4.4	7.7

It is also seen from Figure 10 that Unit E-C80-B80-0 could not reach $\mu = \pm 4$ but other specimens could reach $\mu = \pm 4$ or even larger before the strength degraded to 50% of the maximum measured strength. To evaluate the flexural behaviour of these specimens, their measured beam strengths at the first cycle of $\mu = +4$ were compared. It is obvious that Unit AD-C80-B80I-0 attained the largest strength, followed by the other AD specimen, CD and H specimens”. Table 5 summarises the displacement ductility factor (μ) and drift of these specimens at failure. It can be observed that Unit CD-C80-B80-0 is the most ductile, followed by Units AD-C80-B80I-0, H-C80-B80-0, AD-C80-B80-0 and E-C80-B80-0. A similar trend is observed for the ultimate drift in these specimens.

It is concluded that without axial load, the ductility performance of the “empty joint” is the poorest. Although the joint reinforced with continuous diagonal bars behave fairly ductile, it could not reach the theoretical moment capacity. The performance of joints installed with additional diagonal bars and stirrup were more or less similar in terms of flexural strength and ductility.

4.4 Behaviour of joints with axial load

Similar to Figure 10, Figure 11 shows the column shear force – drift response of Units E-C80-B40-0.2, H-C80I-B80I-0.6, AD-C80I-B80I-0.6, AD-C80I-B80M-0.6 and CD-C80-B40-0.3. These specimens were subjected to compressive axial load with level ranging from 0.2 to 0.6. Except for Unit AD-C80I-B80I-0.6 that failed prematurely outside its critical region (Figure 12), the “empty joint” specimen in this series also had the lowest ductility. Unit E-C80-B40-0.2 suffered joint failure at $\mu = \pm 3$ and the strength enhancement was insignificant as well as unsustainable.

As for Unit AD-C80I-B80I-0.6 the premature failure happened at the weakest region in the middle span of each beam. It has to be noted that this specimen contained extra confinement steel in its beams and columns only near the joint. The same phenomenon did not happen in Unit AD-C80I-B80M-0.6 because the extra confinement steel was provided along the full length of its beams.

It is also evident in Figure 11 that the H and AD specimens have measured flexural strengths larger than their respective theoretical values. Although Unit AD-C80I-B80I-0.6 has the largest strength enhancement, its flexural strength degraded drastically in the second cycle of $\mu = +3$ due to the reason explained before.

Table 6 summarises the flexural strength enhancement ratio, ultimate displacement ductility factor and ultimate drift. It is apparent that the H specimen is the most ductile, followed by the AD specimen containing improved confinement steel along its beams and then by the CD specimen. The other AD specimen performed poorer than the E specimen due to the reason explained earlier.

Table 6. Test results of beam-column joints with axial load

Specimen	M_n (kNm)	Failure mode	Actual/nominal strength ratio	At failure	
				μ	drift (%)
E-C80-B40-0.2	111.8	Joint brittle failure	1.06	3.9	4.4
H-C80I-B80I-0.6	118.8	Beam flexural failure	1.07	5.0	5.4
AD-C80I-B80I-0.6	118.2	Beam shear failure	1.25	3.0	2.9
AD-C80I-B80M-0.6	118.5	Beam flexural failure	1.17	4.8	5.0
CD-C80-B40-0.3	111.6	Local bond failure	1.03	4.7	5.0

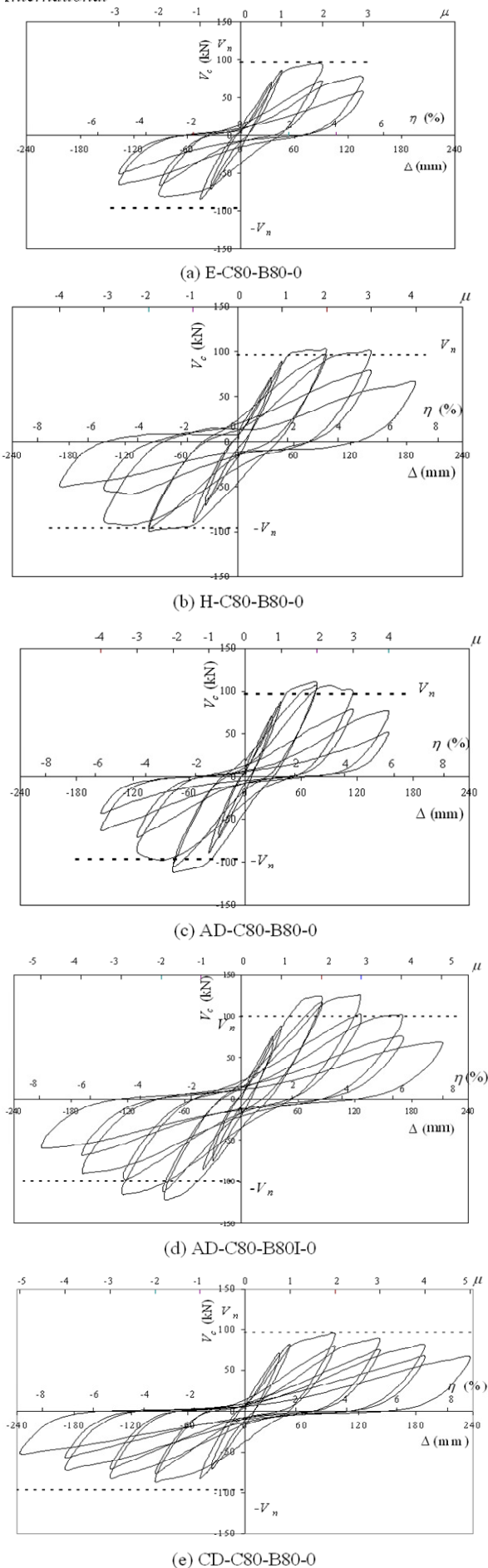


Figure 10. Column shear force – drift response of joint specimens under reversed cyclic loading without axial load

By comparing Tables 5 and 6, it can be shown that in terms of ultimate displacement ductility factor, all the joint specimens without axial load performed worse than their respective counterpart (except for Unit AD-C80I-B80I-0.6 due to premature shear failure as explained previously) subjected to compressive axial load. However, in terms of ultimate drift, all the joint specimens without axial load performed better than their respective counterpart subjected either to moderate or high compressive axial load. As “drift” represents a more realistic deformability than “ductility”, it can be concluded that all the beam-column joint specimens without axial load performed better than those with axial load. This result is contradictory to the commonly accepted theory that compressive axial can improve the performance of beam-column joints [Park & Paulay 1975].

If the performance of the H specimen, with or without axial load, is regarded as behaving in a fully ductile manner suitable for the design in regions with high seismic risk, the performance of the AD (provided with more confinement steel along its beams) and CD specimens, which have ultimate displacement ductility factor and drift slightly less than those of the corresponding H specimen, can be regarded as behaving in a limited ductile manner. As a result, the proposed detailing will be appropriate for the joint design in regions of low-medium seismic risk such as HK.

5 SUMMARY OF PROPOSED DESIGN GUIDELINES

It is hoped that the following proposed design guidelines of HSRC columns and internal beam-column joints could be incorporated into local design practice in the future to improve the column as well as the joint ductility.

5.1 Limited ductile HSRC columns ($f_{cu} \leq 100\text{MPa}$)

A limited ductile HSRC column shall contain transverse steel within its critical region according to Equation (3). The end hooks of transverse steel shall be 135° with an anchorage length of at least 6 times its diameter. Outside the critical region, the transverse steel content can be based on the shear requirement and the end hooks can be 90° .

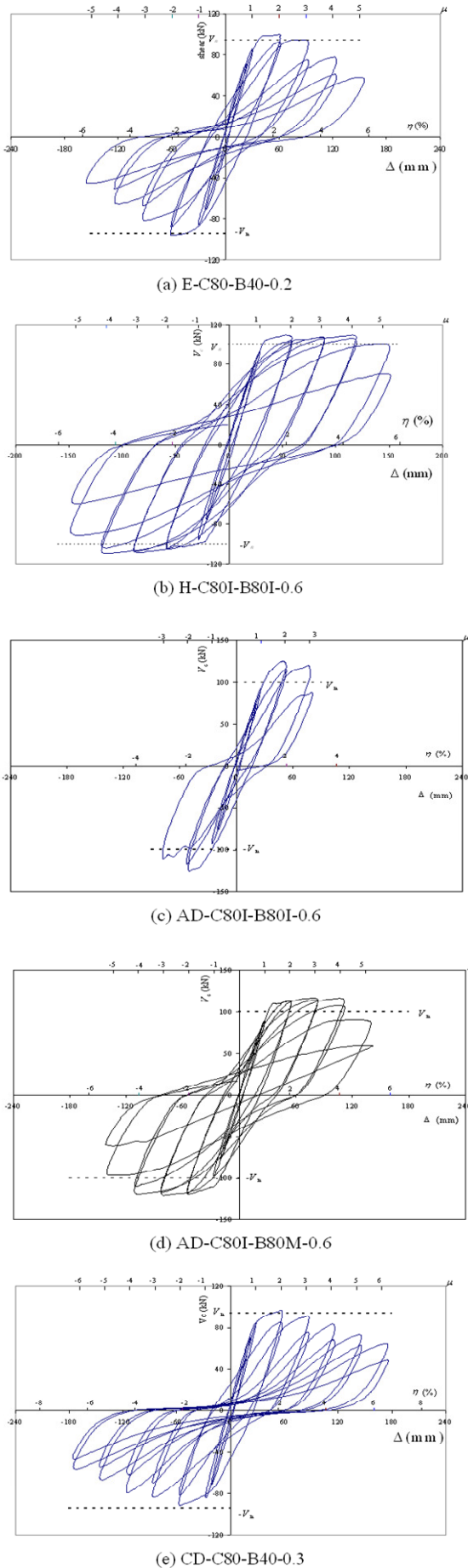


Figure 11. Column shear force – drift response of joint specimens under reversed cyclic loading with axial load

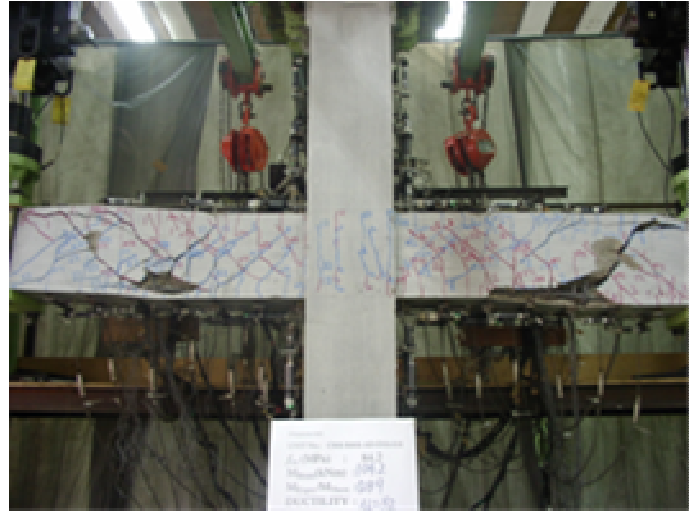


Figure 12. Unit AD-C80I-B80I-0.6 at failure

The extent of critical regions (l_p) shall be measured from the point of maximum moment over a finite length suggested as follows: (1) For $0 \leq P/(A_g f_{cu}) \leq 0.1$, $l_p =$ largest cross-section dimension or where the moment exceeds 0.85 of the maximum moment, whichever is larger; (2) For $0.1 < P/(A_g f_{cu}) \leq 0.3$, $l_p = 1.5$ times the largest cross-section dimension or where the moment exceeds 0.75 of the maximum moment, whichever is larger; and (3) For $0.3 < P/(A_g f_{cu}) \leq 0.6$, $l_p = 2$ times the largest cross-section dimension or where the moment exceeds 0.65 of the maximum moment, whichever is larger. These guidelines for column critical regions have been adopted by the recent HK RC code [BD 2004].

5.2 Internal beam-column joint with additional or continuous diagonal steel ($f_{cu} \leq 80 \text{ MPa}$)

The cross-section area (A_{sh}) of additional/continuous diagonal bars in the joint shall be calculated by:

$$A_{sh} = \frac{V_{sh} \times \gamma_m}{(f_y + \sigma'_s) \times \cos \theta} \quad (5)$$

Where, V_{sh} = shear force taken up by the diagonal steel that can be obtained from the difference between the ultimate joint shear force and the shear contribution from the diagonal concrete strut, $\gamma_m = 1.15$, f_y = yield strength of longitudinal steel, σ'_s = the smaller of the yield strength of additional diagonal steel or 440MPa and θ = inclination of the concrete strut.

The additional diagonal steel shall be provided with sufficient development length but not too long beyond the beam-column interface. The development length of the additional diagonal steel is denoted by l_s (measured from the beam-column interface) and L_s (measured from the intersection of

diagonal bars), which should be respectively determined from the larger of one-half beam depth or one-half its flexural development length and from:

$$L_s \geq \frac{(0.5\alpha_a f_y)}{\sqrt{0.85 f_{cu}}} d_s \quad (6)$$

where $f_{cu} \leq 80\text{MPa}$, $\alpha_a = 1.3$ for top reinforcement where more than 300mm of fresh concrete is cast in the member below the bar or 1.0 for all other cases and d_s = diameter of the additional diagonal steel.

The extent of critical region for columns should follow the guidelines in Section 5.1, and for beams should be the larger of 400mm or 1.5 times the largest cross-section dimension. Ratio between the overall depth of column h_c and the diameter of diagonal steel d_s should satisfy $h_c / d_s \geq 15$.

6 CONCLUSIONS

HKU has been conducting experimental research on the flexural ductility of RC members and joints since 2000 in order to promote earthquake design of RC structures. This paper gives a review on the experimental results obtained for HSRC columns and internal beam-column joints.

HSRC columns (NEW columns) designed according to the proposed equation had flexural strength and ductility superior to the counterpart (BS columns) designed according to BS8110 [1985]. The NEW columns behaved limited ductile in that they could achieve curvature ductility factors of about 10. The test results also showed that the addition of cross ties in the NEW columns increased the column drift.

Tests on internal beam-column joints showed that the "empty" joint had the poorest ductility performance. Joints reinforced with stirrups could improve the flexural ductility with or without axial load. However, such arrangement creates steel congestion problem within the joint and hence causes fabrication difficulties. The proposed joint detailing, both additional and continuous diagonal bars, had ductility larger than that with stirrup without axial load. For joints subjected to medium to high axial load, the joint containing continuous or additional diagonal bars had roughly similar flexural ductility and drift as those of joint with stirrup. The proposed joint details are thus considered to behave limited ductile and appropriate for joint design in regions of low-medium seismic risk like HK.

7 ACKNOWLEDGEMENTS

The work described in this paper has been substantially supported by a grant from the Research Grants Council of the HK Special Administrative Region, China (Project No. HKU 7012/98E & 7125/03E). Technical supports for the experimental tests provided by the laboratory staff of the Department of Civil Engineering, HKU, are gratefully acknowledged.

8 REFERENCES

- Au F.T.K., Huang K. and Pam H.J. (2005), "Performance of interior beam-column joints reinforced with diagonal steel under cyclic loading", *Proceedings, Institution of Civil Engineers, Structures and Buildings*, Vol. 158, Issued SB1, Feb 2005, pp. 21-40. (Erratum of the title: Vol. 158, Issue SB2, April, pp. 155)
- British Standards Institution, BS8110 (1985), "Structural use of concrete", Part 1 *Code of practice for design and construction*, London, U.K.
- Buildings Department (BD) (2004), *Code of Practice for Structural Use of Concrete 2004*, The Government of the Hong Kong Special Administrative Region, August, 180pp.
- GB 50011 (2001), *Code for seismic design of buildings*, National Standard of the PRC, China Architecture and Building Press, Beijing, China, 327pp.
- Ho J.C.M. and Pam H.J. (2002), "Flexural strength and ductility performance of high-strength reinforced concrete columns", *The Structural Engineer*, Vol. 80, No. 23/24, 3 December, pp. 26-34.
- Ho J.C.M. and Pam H.J. (2003), "Inelastic design of low-axially loaded high-strength reinforced concrete columns", *Engineering Structures*, Vol. 25, No. 8, July, pp. 1083-1096.
- Ho J.C.M. (2003), "Inelastic design of reinforced concrete beams and limited ductile high-strength concrete columns", *Ph.D. Thesis*, The University of Hong Kong, Hong Kong, January, 332pp.
- Huang K. (2003), "Design and detailing of diagonally reinforced interior beam-column joints for moderate seismicity regions", *PhD Thesis*, The University of Hong Kong, September, 278pp.
- Li J. (2003), "Effects of diagonal steel bars on performance of interior beam-column joints constructed with high-strength concrete", *Ph.D. Thesis*, The University of Hong Kong, Hong Kong, May, 314pp.
- Mendis P. (2001), "Plastic hinge lengths of normal and high-strength concrete in flexure", *Advances in Structural Engineering*, Vol. 4, No. 4, November, pp. 189-195.
- NZS 3101 (1995), "The design of concrete structures", *Concrete Structures Standard*, Part 1: Code of Practice, Part 2: Commentary, Standards New Zealand, Wellington, New Zealand, 256pp & 264pp.
- Park R. and Paulay T. (1975), *Reinforced Concrete Structures*, John Wiley & Sons, New York, USA, 769pp.
- Watson S. and Park R. (1994), "Simulated seismic load tests on reinforced concrete columns", *Journal of Structural Engineering*, ASCE, Vol. 120, No. 6, June, pp. 1825-1849.